27th Nordic Seminar on Computational Mechanics
NSCM-27
A. Eriksson, A. Kulachenko, M. Mihaescu and G. Tibert (Eds.)

PREDICTION OF THROUGH-THICKNESS STRESS DISTRIBUTION IN LAMINATED SHELL STRUCTURES

J. FRÄMBY*, J. BROUZOULIS, M. FAGERSTRÖM AND R. LARSSON

Department of Applied Mechanics
Chalmers University of Technology, Gothenburg, Sweden
e-mail: framby@chalmers.se, web page: http://www.chalmers.se/am

Key words: Multiscale, FRP, Laminate, Through-thickness stress distribution

1 INTRODUCTION

The ability to, by numerical simulations, investigate the crashworthiness of fibre reinforced polymer (FRP) vehicle structures is crucial for a widespread use of these materials in future cars. Consequently, for an accurate prediction of the crashworthiness performance, crucial failure mechanisms, e.g. initiation and propagation of delamination, needs to be accurately captured in the simulations. However, to enable full car crash Finite Element (FE) analyses in the automotive industry, computational efficiency is essential; therefore, shell elements are mostly used. A drawback of using a shell analysis approach is the low accuracy of the predicted through-thickness distribution of the out-of-plane stress components, which are essential for prediction of delamination initiation.

Aiming to improve the calculated stress distribution while still keeping a shell analysis approach, the current contribution investigates the potential of using a multiscale procedure in order to obtain an improved resolution of the through-thickness stress distribution compared to a pure shell analysis.

First the kinematic description of the shell (the macroscale) is presented. Then the prolongation conditions are described; how the macroscopic deformation measures are used to construct boundary conditions for a detailed 3D Representative Volume Element (RVE) analysis of the laminate. Several types of boundary conditions on the RVE are considered and in order to find the most appropriate type, with respect to accuracy in the through-thickness stress response, a numerical example is presented.

2 MACROSCOPIC KINEMATICS

2.1 Initial shell geometry and convected coordinates

As a staring point, a point $\boldsymbol{X}$ in the initial configuration B_0 of the shell is described by the placement map $\boldsymbol{\Phi}(\boldsymbol{\xi}) \in \mathcal{B}_0$ parametrised in terms of convected (covariant) coordinates $\boldsymbol{\xi} = (\xi_1, \xi_2, \xi)$ as

$$\boldsymbol{X}(\boldsymbol{\xi}) = \boldsymbol{\Phi}(\boldsymbol{\xi}) = \boldsymbol{\Phi}_0(\boldsymbol{\xi}_0) + \xi \boldsymbol{M}(\boldsymbol{\xi}_0) \tag{1}$$

where $\boldsymbol{\xi}_0 = (\xi_1, \xi_2)$. The mapping $\boldsymbol{\Phi}(\boldsymbol{\xi})$ is defined by the midsurface placement $\boldsymbol{\Phi}_0$ and the outward unit normal vector field $\boldsymbol{M}$, where the coordinate $\xi \in \frac{h_0}{2}[-1, 1]$ is associated with this

direction and h_0 is the initial thickness of the shell. The covariant basis vectors are defined as

$$\boldsymbol{G}_\alpha = \boldsymbol{\Phi}_{0,\alpha} + \xi \boldsymbol{M}_{,\alpha}; \quad \alpha = 1,2; \qquad \boldsymbol{G}_3 = \boldsymbol{M} \tag{2}$$

where $\bullet_{,\alpha}$ denotes the derivative with respect to ξ_α.

2.2 Current shell geometry

A point, $\boldsymbol{x}$, in the current (deformed) configuration $\mathcal{B}$ is described by the deformation map $\boldsymbol{\varphi}(\boldsymbol{\xi}) \in \mathcal{B}$ of the inertial Cartesian frame as

$$\boldsymbol{x}(\boldsymbol{\xi}) = \boldsymbol{\varphi}(\boldsymbol{\xi}) = \boldsymbol{\varphi}_0(\boldsymbol{\xi}_0) + \xi \boldsymbol{m}(\boldsymbol{\xi}_0) + \frac{1}{2}\xi^2 \gamma(\boldsymbol{\xi}_0)\boldsymbol{m}(\boldsymbol{\xi}_0) \tag{3}$$

where the mapping is defined by the midsurface placement $\boldsymbol{\varphi}_0$, the spatial director field $\boldsymbol{m}$ and an additional scalar thickness inhomogeneity strain γ, *cf.* also Figure 1.

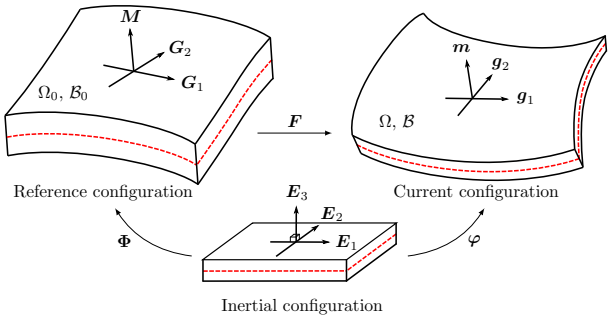

Figure 1: Mappings of shell model defining undeformed and deformed shell configurations relative to inertial Cartesian frame.

The pertinent spatial covariant basis vectors are given as

$$\boldsymbol{g}_\alpha = \boldsymbol{\varphi}_{0,\alpha} + \left(\xi + \frac{1}{2}\gamma\xi^2\right)\boldsymbol{m}_{,\alpha} + \frac{1}{2}\gamma_{,\alpha}\xi^2\boldsymbol{m}; \quad \alpha = 1,2; \qquad \boldsymbol{g}_3 = (1+\gamma\xi)\,\boldsymbol{m} \tag{4}$$

3 COUPLING BETWEEN THE SCALES – PROLONGATION

In order to couple the macroscopic scale with the laminate level, relations between the kinematics on the two scales must be established. Following Larsson and Landervik[1], it is assumed that the averaged deformation field varies slowly enough within the RVE to justify that it is constant in the *tangent* plane (=) of the shell. In the thickness ($\perp$) direction separation of micro- and macro scales cannot be assumed, whereby the microscopic fluctuations on the laminate level must be completely resolved in the thickness direction. Thus, the thickness of the RVE is given by the thickness of the thin-walled structure,whereas the in-plane extensions of the RVE should be chosen based on a balance between accuracy and computational efficiency. In the following, we consider quantities related to the macroscopic fields denoted by a superimposed bar, *e.g.* $\bar{\bullet}$.

3.1 Kinematic expansions of macroscopic fields in the RVE

The particular expansion used to describe the relative placement field inside the RVE is decomposed into separate portions in the tangent- and thickness direction, $\bar{\boldsymbol{x}}_{=}$ and $\bar{\boldsymbol{x}}_{\perp}$ respectively. Thus, the relative placement $\Delta\boldsymbol{x}(\boldsymbol{X})$ (measured as the placement relative to the expansion point $\bar{\boldsymbol{X}}$) can be expressed as

$$\Delta\boldsymbol{x} = \Delta\bar{\boldsymbol{x}}_{=} + \Delta\bar{\boldsymbol{x}}_{\perp} + \boldsymbol{u}_{\mathrm{f}} \tag{5}$$

where $\boldsymbol{u}_{\mathrm{f}}$ is the laminate level displacement field. As to the particular descriptions of the placement fields, different Taylor series expansions are used. The tangent placement, $\Delta\overline{\boldsymbol{x}}_{=}$, is defined by a first order expansion, at each ξ-level in the ξ_α directions, of the RVE defined as

$$\Delta\overline{\boldsymbol{x}}_{=} = \overline{\boldsymbol{g}}_{\alpha|\xi}\Delta\xi_\alpha \tag{6}$$

where the notation $\overline{\boldsymbol{g}}_{\alpha|\xi}$ implies that the expansion is made for a fixed value of ξ. The placement in the thickness direction, $\Delta\bar{\boldsymbol{x}}_{\perp}$, is formulated as the second-order Taylor series expansion (involving the second gradient $\overline{\boldsymbol{K}} = (\overline{\boldsymbol{g}}_i \otimes \overline{\boldsymbol{G}}^i)_{,j} \otimes \overline{\boldsymbol{G}}^j$) about the *origin* of the RVE as

$$\Delta\overline{\boldsymbol{x}}_{\perp} = \overline{\boldsymbol{g}}_{3|\xi=0}\xi + \frac{1}{2}\overline{\boldsymbol{g}}_{3,3|\xi=0}\xi^2 \tag{7}$$

For further details about the prolongation procedure, see[1].

3.2 Choice of boundary conditions

The boundary conditions for the RVE analysis need to be chosen with due consideration to the adopted homogenisation procedure. In this contribution different boundary conditions have been studied: (i) *Mixed* boundary condition – Dirichlet boundary conditions are applied on the in-plane surfaces of the RVE, *i.e.* $\boldsymbol{u}_{\mathrm{f}} = \boldsymbol{0}$ and Neumann (traction free) conditions on the top and bottom surface; (ii) pure *Dirichlet*, with all six surfaces of the RVE subjected to the condition $\mathbf{u}_{\mathrm{f}} = \mathbf{0}$; (iii) *Taylor* boundary conditions, *i.e.* the fluctuation field $\mathbf{u}_{\mathrm{f}} = \mathbf{0}$ in the entire domain; .

4 NUMERICAL EXAMPLE

A square isotropic plate, clamped at one edge and subjected to a prescribed edge displacement on the opposite edge has been simulated using the described shell model and a 3D continuum solid model (reference case) using a hexahedron element mesh. To compare the results from the two models a shell integration point close to the middle of the plate has been chosen. At this point the generalised strains of the shell model are extracted, *i.e.* $\bar{\boldsymbol{g}}_{\alpha|\xi}$, $\bar{\boldsymbol{m}}$ and $\bar{\gamma}$, such that the proper displacement can be applied to the RVE according to Eq. (5) (and particular choice of boundary condition). The corresponding stress distribution inside the RVE can then be solved for.

In Figure 2, the computed stress distribution for component σ_{xz} is shown for the: solid model; shell model; and RVE:s with different in-plane sizes as well as different boundary conditions. As can bee seen in Figure 2a, an increased RVE size does not converge towards the reference model; only a qualitative improvement in terms of shape is observed. This implies that an increase in RVE size leads to an increased deviation in the applied shear deformation (on the RVE)

compared to both the reference and the shell model. The effect from different RVE boundary conditions on the stress distribution is shown in Figure 2b. It can be seen that when *Dirichlet* or *Taylor* boundary conditions are applied, the results are similar to that of the shell. Furthermore, the *Mixed* boundary condition fulfills the traction free condtion on the top an bottom surface, although the maximum stress is underestimated.

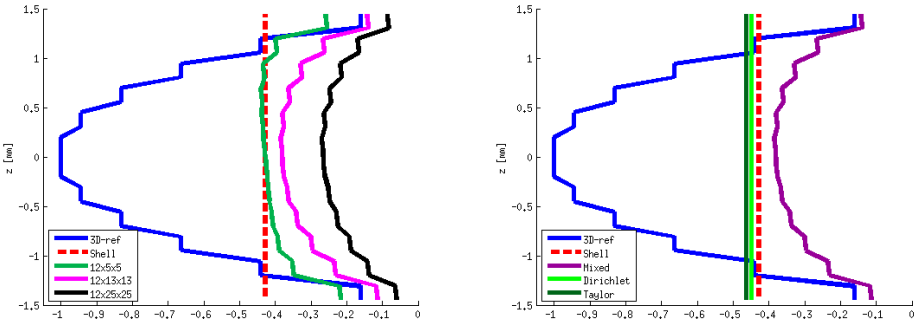

(a) (b)

Figure 2: Comparison of out-of-plane shear stress distribution, σ_{xz}, through the thickness. (a) Comparison between different in-plane RVE-sizes (for *Mixed* boundary conditions). (b) Different types of boundary conditions (illustrated on a 12x13x13 element RVE).

5 CONCLUSIONS

In this contribution, the potential of using a multiscale approach for increasing the accuracy of the stress components has been studied. Different boundary conditions on the RVE have been investigated and in the case of an isotropic plate, the results show that the size of the RVE cannot be chosen too large as this will lead to non-matching deformation modes on the two scales. In the anisotropic case (transverserly isotropic laminae), similar conclusions can be drawn (not shown here). Moreover, results indicate that the 'best' obtainable stress distribution (compared to the reference case) corresponds to what is obtained in the shell analysis. In particular, the stress distribution obtained in the pure shell analysis is recovered for the case of Taylor and Dirichlet boundary conditions. In addition to described boundary conditions, weak periodic boundary conditions have also been studied and will be presented. To accomplish results closer to the reference case with the given multiscale method, a higher order expansion of the relative placement would likely be necessary.

Finally, an alternative post-processing recovery approach to obtain the through-thickness stress distribution, based on the integration of the momentum balance equations, has also been investigated. Initial results (not shown here) indicate that for the isotropic case, the distributions correlate well with the reference case. These results and results for a laminate with transversely isotropic properties will be presented.

REFERENCES

[1] Larsson, R. & Landervik, M. A stress-resultant shell theory based on multiscale homogenization. *Computer Methods in Appplied Mechanics and Engineering* **263**, 1–11 (2013).